

# LIZARD: Pervasive Sensing for Autonomous Plastic Litter Monitoring

Farooq Dar  
*University of Tartu*  
farooq.dar@ut.ee

Agustin Zuniga  
*University of Helsinki*  
agustin.zuniga@helsinki.fi

Mayowa Olapade  
*University of Tartu*  
mayowa.olapade@ut.ee

Monica Passananti  
*University of Turin*  
*University of Helsinki*  
monica.passananti@unito.it

Abdul-Rasheed Ottun  
*University of Tartu*  
ottun@ut.ee

Sasu Tarkoma  
*University of Helsinki*  
sasu.tarkoma@helsinki.fi

Zhigang Yin  
*University of Tartu*  
zhigang.yin@ut.ee

Petteri Nurmi  
*University of Helsinki*  
petteri.nurmi@helsinki.fi

Mohan Liyanage  
*University of Tartu*  
mohan.liyanage@ut.ee

Huber Flores  
*University of Tartu*  
huber.flores@ut.ee

**Abstract**—Littering is a significant environmental concern that causes significant damage to the natural ecosystem and contributes adversely to human health. Monitoring litter accumulation is currently labour-intensive and costly, often resulting in action being taken only once the environment has already become polluted. We contribute LIZARD, a novel pervasive sensing solution for detecting and monitoring plastics that is tailored to autonomous vehicles. LIZARD relies on an innovative sensing pipeline that combines thermal imaging and optical sensing. The intuition is to rely on thermal dissipation patterns to identify larger (macro) plastics and use optical sensing to sample area with the highest density of plastics to identify smaller (micro and meso) plastics. Ours is the first pervasive sensing solution that can detect microplastics in the environment and be integrated into autonomous vehicles. Indeed, state-of-the-art solutions are either limited to laboratory analysis with special instruments or rely on manual observation without being able to identify the smallest plastics – which often are the most dangerous. We evaluate LIZARD through rigorous experiments that combine controlled laboratory settings and in-the-field measurements carried out in three real-world locations to evaluate LIZARD. Our results show that LIZARD can be used to detect plastics of different sizes with an accuracy of up to 80%. The performance depends on the diameter of the plastics, the background surface, and the luminosity of the environment. We also demonstrate that our solution can be easily integrated with ground drones, enabling (semi-)autonomous litter monitoring. Our work offers an innovative way to harness pervasive sensing to address an important global (environmental) sustainability challenge while paving the way toward improved monitoring of the accumulation of harmful plastic fragments in the environment.

**Index Terms**—Drones, IoT, Visual inspection, Light reflectivity

## I. INTRODUCTION

Littering resulting from human activity is a major concern, particularly in highly populated areas, that results from deficient human practices, poor garbage collection systems, and lack of limited awareness about the problem [1], [2]. The adverse effects of litter are numerous, ranging from damage to the natural ecosystem to contributing to human health [3], [4]. For instance, litter particles can be ingested by birds, dogs, or other animals, resulting in the litter entering the global food chain [5], [6]. The main problem with litter pollution is that once it is introduced into the environment, it is difficult to remove it

completely. Most types of litter can persist for long periods of time in the environment and even blend with the soil or other parts of the ecosystem as time elapses. Moreover, many litter objects do not decompose naturally (e.g., plastics), instead breaking into smaller pieces due to environmental degradation, human activity, weather, or other factors. As a result, litter is not only an important but also a challenging problem to tackle.

Detecting small litter fragments is essential for mitigating long-term adverse effects of pollution, yet currently, no scalable, cost-effective, and accurate solutions exist. State-of-the-art solutions for detecting litter rely on specialized measurement instruments, such as spectroscopy, on samples collected from a specific location. These, however, cannot be integrated into end devices nor support end-users as they require specialized expert knowledge and skills [7]. Thus, instead, the most common approach for litter removal is to rely on human activity, either volunteers or contract workers. This approach is best suited for recently deposited litter as litter is mostly identified using (manual) visual inspection, which works best for materials that are intact and that have not blended with the environment [8]. These activities can be effective when performed regularly – i.e., before the litter objects break. However, these activities are costly, require strong planning and logistics. Thus, they are not scalable as a long term solution. Also, some technological solutions for facilitating litter cleanup have been proposed, such as autonomous sweepers [9] or aerial UAVs that identify litter [10]. However, these are limited to large litter objects that are easy to spot. Additional sensing technologies can aid these solutions to make them more effective. For instance, mounting a camera in a vehicle to identify litter in a location using object recognition techniques. These solutions are equally difficult to deploy at scale and are unable to detect harmful litter fragments, such as micro (diameter < 5mm) or meso particles (diameter 5-10mm) [11]. Indeed, object detection techniques have limited discriminatory power and are too difficult to apply to identify intrinsic properties of objects that have lost their shape and form, e.g., fragments of a broken bottle.

We contribute LIZARD, a novel and innovative pervasive sensing solution for monitoring plastic litter. LIZARD identifies

both larger (macro) litter and smaller plastic fragments (micro and meso plastics). We focus specifically on plastics, as they have been identified as one of the most significant environmental hazards due to their widespread use and lack of decomposition. Indeed, microplastics have recently been identified as a significant health concern, and most microplastics originate from ground litter. LIZARD builds on an innovative pervasive sensing approach that combines two complementary sensing modalities, thermal imaging and optical sensing, using light reflectivity. These modalities are well-suited for autonomous monitoring as they can operate using lightweight machine-learning models, unlike computer vision, which requires complex and power-hungry models. LIZARD first analyzes sunlight-induced thermal characteristics of objects using thermal imaging. As thermal radiation fades when the size of the object becomes smaller, LIZARD relies on a second sensing modality based on light reflectivity to explore the existence of smaller litter fragments in the environment. As light reflectivity is sensitive to ambient luminosity, it requires close contact with litter to be effective. To overcome this limitation, LIZARD harnesses the thermal imaging analysis to determine the optimal area to sample with optical sensing, and then uses close contact light reflectivity sensing on this area. This reduces the time that light reflectivity needs to be used, and reduces the overall energy drain of the method by reducing the overall mapping effort. We evaluate LIZARD through extensive and rigorous experiments that combine controlled laboratory experiments and real-world deployments conducted in three real-world locations. Our results indicate that LIZARD can accurately detect three different types of litter (micro, meso, and macro). We also demonstrate how LIZARD is easy to integrate with off-the-shelf (autonomous) ground drones, making it possible to adopt LIZARD for autonomous litter monitoring. Our work paves the way towards new innovative mechanisms for improving environmental sustainability and mitigating the adverse effects of littering by offering a solution that extends on current solutions by detecting both large plastic litter (macro) and smaller litter fragments (micro and meso), and that can be integrated with autonomous ground vehicles.

## II. MOTIVATION

The most common automated approach for supporting litter detection is vision-based object detection [12]. This approach suffers from poor accuracy when deployed in the wild, being mostly limited to larger and intact litter objects, and being power hungry, making it difficult to use this approach as part of constrained devices, such as drones. We demonstrate that plastic identification solutions can be integrated into AGVs using lightweight thermal sensing. Thermal imaging has been shown as a promising technology to characterize the material of different litter objects [13] and it can exploit (opportunistic) heat sources (such as the sun) to reduce the cost of the sensing process [14]. We show that these methods can improve the detection and removal of plastics by identifying the appropriate material ensuring proper recycling can be applied.

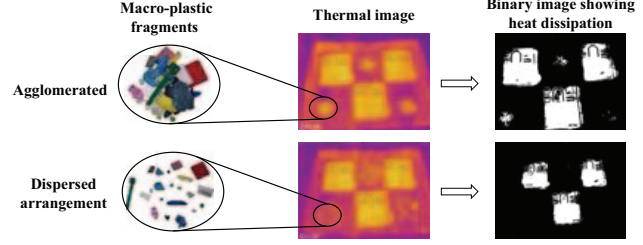


Fig. 1: Combination of macro-plastics and micro-plastics (agglomerated and dispersed).

**Testbed:** We conduct experiments measuring the thermal dissipation time of plastics of different sizes: macro-scale (diameter > 10mm), meso-scale (5 – 10mm) and micro-scale (< 5mm). For the macro-scale, we focus on plastic objects and rely on specialized samples that have been produced following a consistent manufacturing process, as this ensures that objects are comparable and thermal radiation differences correspond to the polymer. Thermal radiation is induced using a bulb of 60 W as a heat source. For the micro and meso-scale, we consider plastic samples extracted directly from the environment. Section IV describes these samples. Janeli Incubator is used to induce thermal radiation in the samples as it allows inducing a consistent amount of thermal radiation. An off-the-shelf smartphone FLIR CAT S61 is used as the thermal sensing unit in the experiments.

**Procedure:** Plastic samples are exposed to an ambient temperature ranging between 22 °C to 24 °C before starting the experiment. Next, each sample is located over a matte black surface, and the lamp is placed at a fixed distance of 10 cm from the samples to avoid burn damage while ensuring they are exposed to sufficient amounts of thermal radiation. The black surface ensures consistent measurements across the samples as it absorbs additional thermal radiation. We consider four heating durations (1, 2, 3 and 4 minutes) that correspond to differing initial temperatures and measure the dissipation of the thermal footprint. Similarly, micro and meso samples are put inside the incubator for about 15 minutes at a temperature of 30 °C. To verify that enough thermal radiation was induced to the plastic fragments by the incubator, we also included the macro samples in the experiment. Figure 1 shows the arrangement of samples. In addition, we consider two types of arrangements for the plastic fragments: agglomerated (AA) and dispersed (DA). In the former, samples overlap each other so that thermal radiation transfers between samples. In the latter, the fragments are separated from each other.

**Results:** Figure 2 shows that the thermal dissipation time of the plastic samples can be used to detect the type of material. Friedman test using plastic type and thermal dissipation time as experimental condition shows the differences between plastics materials to be statistically significant ( $\chi^2(2) = 61.47$ ,  $p < .05$ ,  $W = 0.80$ ), demonstrating that thermal radiation can indeed characterize different plastics. While thermal radiation is easily measured for macro plastics, Figures 2(e-f) shows that the same analysis cannot be repeated for plastic fragments. From

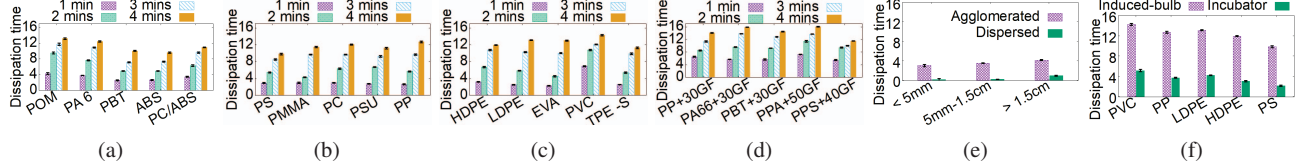


Fig. 2: Thermal dissipation times(min) for (a-d) 20 samples, (e) Micro and meso plastics, and (f) Selected macro plastics.

Figure 2e, we can observe that when fragments are overlapping (agglomerated), there is sufficient thermal radiation to obtain a thermal footprint. However, particularly when the samples come from different materials, it becomes difficult to determine the material precisely. When the fragments are dispersed, then the amount of thermal radiation is insufficient for obtaining a footprint. We separately assessed the thermal dissipation times of the macro samples when the incubator was used as a heat source, and the results showed that the thermal dissipation times followed the same relative trend compared to using the bulb as a thermal radiation source (Figure 2f). Kolmogorov-Smirnov test comparing relative differences in thermal dissipation time verified that the times are similar in both cases ( $KS=0.2$ ,  $p > 0.05$ ). This indicates that the heat does not need to be evenly distributed along the object but that even a smaller region with consistent heat points is sufficient for detecting plastics.

**Insights:** Our results demonstrate that thermal dissipation time can be used to characterize macro plastics samples, but it fails when identifying smaller plastic fragments. Indeed, micro and meso samples can be characterized barely when they are agglomerated, which is very unlikely to be found in the wild (as we will demonstrate in our main experiments in Section IV). Thus, individual modalities alone are insufficient for detecting plastics of different scales. LIZARD overcomes this challenge by innovatively combining two complementary sensing modalities.

### III. LIZARD SENSING PIPELINE

LIZARD has been designed to enable autonomous monitoring of litter. Achieving this task, however, is far from straightforward, as the operations need to be sufficiently lightweight so that they do not hamper the primary operations of the drone, and as the detection needs to work robustly across different surfaces and weather conditions. Indeed, the primary focus of ground drones is on autonomous navigation and movement, which means that any auxiliary tasks, such as litter monitoring, must operate with minimal resource consumption. In addition, the technology used for detecting litter needs to be able to work robustly regardless of the surface where litter is placed or the prevailing weather conditions. LIZARD overcomes these challenges by using two complementary sensing modalities and a two-phase sensing pipeline that minimizes unnecessary processing. The overall pipeline is summarized in Figure 3. LIZARD first uses a thermal camera to monitor thermal dissipation patterns and to identify larger macro fragments. This process produces a region of interest (ROI) which is then analyzed with light sensing in more detail using an adaptive sampling scheme designed to minimize excess processing. We next detail these phases.

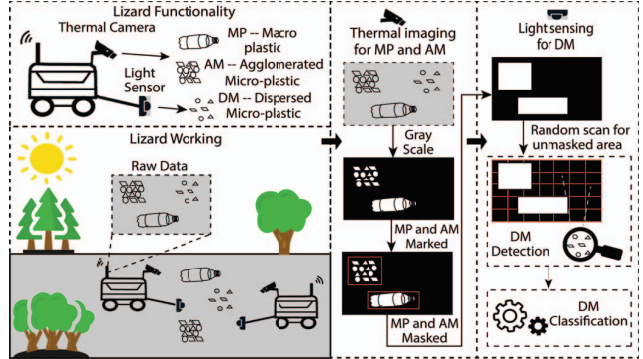


Fig. 3: Plastic fragment sensing and monitoring pipeline.

#### A. Phase 1 - Thermal imaging

**Pre-processing:** In the first phase, video footage is recorded using a thermal camera. Video footage is then converted into a set of sequential images (gray-scale) to perform further pre-processing. Using a gray-scale conversion helps to isolate the background and to segment the image to different objects. The gray-scale image is then smoothed by applying Gaussian-Blur which reduces thermal noise, resulting from low resolution and inaccuracies in the camera. The image is then converted into binary image (0-255) such that thermal dissipation time can be estimated. This makes it possible to isolate the heat sources that are visible as thermal footprints in the images. To aid further the process of highlighting the thermal footprint, each image is enhanced using Adaptive Histogram Equalization technique to enhance the definitions of edges in an image. These steps are summarized in Algorithm 1 (steps 1-3) and are in line with best practices on processing thermal images [13], [15].

**Reducing sampling area:** Since macro litter can be easily detected through thermal imaging, we next focus on the unexplored area to further check the presence of smaller plastic fragments in the environment. Given that mapping an overall area for plastic fragments can be a resource-intensive task not suitable for constrained devices, we first focus on reducing the possible area of exploration. Note that in practice moving the AGV is the most resource-intensive operation. The sensing components of LIZARD are envisioned to operate as a separate payload that incorporates their own power source and computing resources and thus we focus solely on optimizing the resource consumption of the sensing pipeline. Indeed, current AGVs rarely support integration with external components or offer extensive programmability, and thus a separate payload is the most feasible option for integration (see the discussion).

The key technical challenge is how to reduce the area being analyzed in detail as the size of the area directly influences

resource consumption. We first remove areas where macro litter was identified as these areas would already be marked for cleaning regardless. Thus, we are interested in specific places covered by plastic fragments that can potentially remain in the environment - even after cleaning. Binary images thus are processed further by removing the heat source areas that were transformed into binary white parts. These heated parts are detected as white parts and are extracted using Contour Approximation Method from OpenCV. Once the macro litter parts are found using contours, we prepare a patch that is used to mask these large samples in Algorithm 1 (lines 4 to 13). These patches are where the sampling is not required as these areas do not contain any plastic fragments and thus, the sampling area is reduced.

---

**Algorithm 1:** Reduce sampling area of sensing and calculate ROI coordinates

---

```

Data: ThermalImage containing plastic fragments
Result: patch; coordinates of plastic fragment ROIs
1 image  $\leftarrow$  Conversion to Grayscale;
2 image  $\leftarrow$  Apply GaussianBlur;
3 image  $\leftarrow$  Convert to Binary(0 or 255);
4 c  $\leftarrow$  Detect all contours from image;
5 initialize contourarea;
6 for each contour in c do
7   contourarea  $\leftarrow$  area of each contour;
8   area90thquantile  $\leftarrow$  90th quantile of
     contourarea;
9   if contourarea > area90thquantile then
10    | patch  $\leftarrow$  contour Bounding Box Coordinates;
11    | apply bounding box patch on image ;
12   end
13 end
14 ROI  $\leftarrow$  calculate ROIs from remaining sampling area;
15 RandomSample  $\leftarrow$  Random sample from ROIs;
16 BoundingBox  $\leftarrow$  Bounding box of RandomSample;
17 centroid  $\leftarrow$  Centroid of BoundingBox;
18 coordinates  $\leftarrow$  Coordinates of centroid;
19 return coordinates of centroid
```

---

### B. Phase 2 - Light reflectivity

**Defining ROI mapping area:** Next, we define regions of interests (ROI)s in the remaining unexplored area. To do this, we divide the area into multiple ROIs of same height and width. Similar method has been successfully applied to produce images from different resolutions [16], but in our case, we are using it to define the areas to sample. We then calculate the coordinates of these small ROIs to be used for sensing. The key idea is that sampling is carried on within these small areas. To do this, we calculate the ROIs from the remaining unexplored area using a Canny Edge Detection method in OpenCV over the thermal image. The Canny Edge Detection technique isolates the boundaries of plastic fragments. After this, we perform another technique called Morphological Transformation (dilation) to add more pixels to the boundaries

in the image. Another reason to perform dilation on boundaries is because sometimes the boundaries are only visible partially, and we perform dilation to interpolate the missing boundaries (if any) in the image. As a result, the boundaries of the plastic fragment samples become more visible and thicker. Then we mask the large plastic samples from the image using the patch generated previously in Algorithm 1. Once we have the boundaries of the plastic fragment samples, we use Contour detection to extract the ROI area.

**Scheduling light sampling and classification:** The longer the monitoring can operate, the larger the area that can be covered and the better litter can be identified. Movements of the ground vehicle and actuators, such as robotic arms, connected to it result in the highest power drain and thus the monitoring time depends on the area that is sampled. Optimizing the trade-off between monitoring accuracy and cost of ground drone movements is a key challenge for LIZARD and we overcome this issue by using an adaptive sampling area that analyzes the ROI to determine the areas where light reflectivity sampling should be carried out. Since the extracted ROIs may also include noise depending on the background; we perform random sampling on the extracted ROIs (contours in our case). Random sampling is done to minimize the cost of sensing and monitoring. Once random sample is generated, we calculate the centroid of the bounding box enclosing our region of interest and pass the coordinates to the light reflectivity sensor for sensing and monitoring as shown in Algorithm 1 (lines 17-19).

**Sampling robustness:** Since micro-plastics can be found in any area, another important challenge for LIZARD is to operate robustly in different environmental backgrounds. Some locations may be more difficult to map rather than others due to environmental factors, e.g., dirt, humidity, and wind to mention some. Thus, to improve the identification of sampled data, we perform wavelet transform [17] on the sensor data to enrich it and denoise it. The transform includes filtering, thresholding, and scaling of light values. The scaling is performed to generate wavelet coefficients at different scales for performing multiresolution analysis. We then employ change point detection to analyze the reconstructed light sensor data. We use the *roerich* to perform change point detection based on density ratio estimation [18]. We specify the sliding window size, and the result of the change point detection includes the detected change points and the magnitude of change points as shown in Figure 4. These detected change points denote the presence of plastic fragments, and the change point magnitude denotes the type of plastic. The PR-AUC for true change points and predicted change points was around 0.94 (precision: 0.88; recall: 1.0). In addition, as part of our pipeline, when light samples are taken from a ROI, denoised and preprocessed; these samples are then passed to classical machine learning models, such that it is possible to identify the type of the plastic fragment. LIZARD implements Random Forests (RF) and Support Vector Machines (SVM) to support the classification of plastic fragments.

**Technical challenges:** LIZARD combines thermal imaging

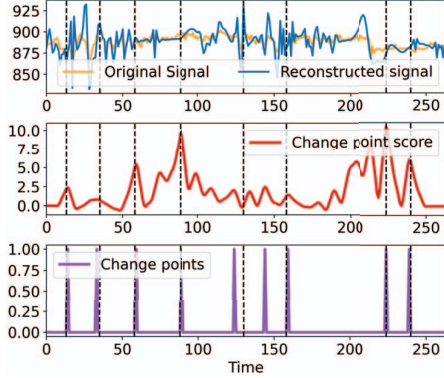


Fig. 4: Wavelet transformation of light sensor data, change point scores and change point detection.

for detecting large plastic fragments and light reflectivity for smaller particles. This combination addresses a major challenge related to the cost of exploring entire areas using sensors. LIZARD also implements an enrichment method to improve the robustness of micro-plastic identification in different environments. Other challenges also include hardware design, sensor placement, field of view, and sensor calibration. Besides this, dynamic adaptation of environmental factors is also a critical problem to overcome for effective operation in the wild. Currently, LIZARD performs efficiently in various environments, providing core functionality that can be easily extended.

#### IV. EXPERIMENTAL SETUP

We evaluate LIZARD through rigorous experiments to show the performance of our method to identify plastic fragments. We begin with controlled experiments that demonstrate how light reflectivity can be used to characterize plastic fragments that were collected from a real environment and proceed to demonstrate how our method can be applied to identify plastic fragments that are dispersed in the wild.

**Apparatus:** We used an off-the-shelf Caterpillar smartphone (CAT). We also use a JANOEL18S incubator as heat source to induce thermal radiation to the plastic samples. As light reflectivity source, we used red light diodes and photoresistors (wavelength 650 nm). We developed an array of 15 light sensors to map an area simultaneously from an autonomous vehicle.

**Plastic samples:** We used plastic fragment samples collected in the wild through a specialized process [19]. These samples are categorized into three different types as shown in Figure 5A, Type 1 ( $< 5$  mm), Type 2 ( $> 5$  mm and  $\leq 15$  mm) and Type 3 ( $> 15$  mm). Type 1 corresponds to micro-plastics, whereas Type 2 corresponds to meso plastics. These two categories are the most dangerous ones as micro-plastics can be easily ingested by animals or be transported to aquatic environments where they enter the food cycle [20]. Meso-plastics, in turn, are fragments that typically are in the process of breaking down into smaller pieces and thus are a source of future micro-plastics. Type 3 effectively corresponds to macro-plastics. Macro plastic samples from end products are also considered in

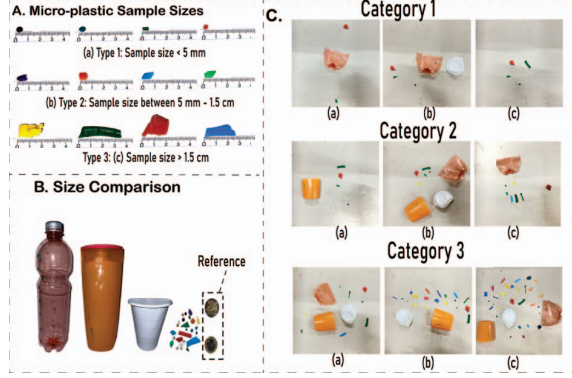


Fig. 5: A. plastic types: (a) 1: Micro ( $< 5$  mm), (b) 2: Meso (5 mm to 15mm), and (c) 3: Macro plastics ( $> 15$  mm); B. Plastic size comparison using coins as a reference; C. Arrangements of micro, meso, and macro plastic samples used in our analysis.

the experiment. As shown in Figure 5B, we used a plastic bottle (PET), a shampoo bottle (HDPE), and a disposable plastic cup (PP). These samples are used together to produce arrangements of deposited plastic litter to be analyzed at once.

**Sample arrangements:** To evaluate whether it is possible to detect plastic fragments in the environment, we first analyze their natural distribution in different environments. We achieve this by analyzing the TACO dataset [21]. TACO is a publicly available image dataset depicting litter in the wild. The dataset contains over 5,000 images of litter ranging from macro to micro sizes. To analyze how micro litter is distributed in the environment, we extract the images from the dataset containing micro and mesolitter. The main goal of this analysis is to establish typical arrangements of plastic fragments, such that those can be analyzed by our method in a controlled manner. Arrangements used in the experiments are shown in Figure 5c and divided into three categories (see Section V for further details about the categories).

**Procedure:** After arrangements of plastic fragments are identified, these are then replicated in a controlled testbed. We develop an exploration area with different backgrounds to which the arrangements are mapped. Arrangements are normalized such that they can be easily mapped into an area of 20 by 14 cm. Once the arrangements are located in the exploration area, this is put into the incubator to induce thermal radiation heat on the samples. After that, the exploration area is removed from the incubator, such that the LIZARD pipeline is applied.

**Design:** There is a large range of available options to integrate LIZARD onto AGVs. Figure 6 shows potential designs and highlights the components that need to be added to the AGVs. One option is to install a simple sun-shield and to use thermal imaging [14], another is to rely on computer vision (Figure 6(c)). Alternatively, light sensors can be integrated into the lower part of the AGV to take light reflectivity measurements (Figure 6(d-e)). We consider a fixedly deployed array of sensors (Figure 6(d)) as we focus on evaluating the sensing performance, but in practice, a robotic hand would be preferred as it would support removing some of the plastic

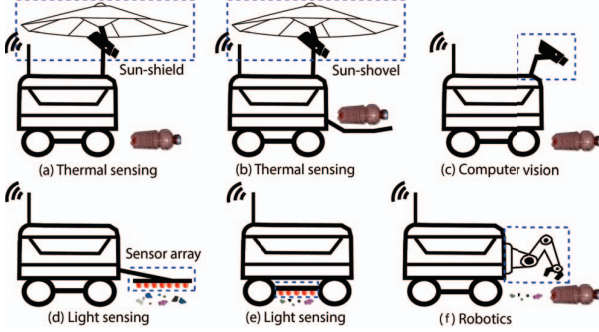


Fig. 6: Lizard design alternatives.

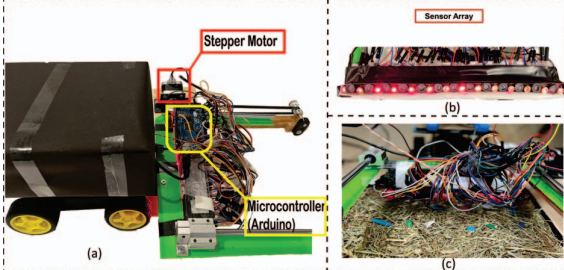


Fig. 7: Lizard prototype, (a) Main Components; (b) Underlying Sensor array; (c) Lizard in action

fragments also. We used light-dependent resistors (LDR) as the sensors, which are sufficient for our purpose.

**Implementation:** We have implemented a proof-of-concept pipeline that has been integrated with a commercial-off-the-shelf AGV. Our working prototype is shown in Figure 7, and its multiple components are highlighted in the figure. Our prototype uses a sensor array that contains 15 light sensors. The distance between the sensors is roughly 1.5 cm, and the sensor array can map an area of  $20 \times 14 \text{ cm}^2$ . The sensor array is mounted on an arm with a linear guide slider, so it is possible to move the array back and forth with a stepper motor (NEMA17). Each light sensor output is connected to analog input pins (pin 1 to 15) of the Arduino Mega ADK microcontroller. The photoresistors connected to the light sensor capture the light intensity of the reflected light by measuring its resistance. Algorithm 1 performs the mapping of coordinates between the ROIs in the image, and the area mapped by the sensor array. The sensor array moves to the appropriate locations and activates the light sensor to collect data in that location. The movements of the sensor array are controlled by the stepper motor driver (A4988), which is also connected to the Arduino microcontroller. Once the samples are taken, these are uploaded to a web server with a timestamp for further analysis.

## V. RESULTS

**Light reflectivity performance:** We first show the performance of the proposed light reflectivity approach when it is used from different distances to identify different types of litter fragments (plastics). Figure 8 shows the results when sampling from a distance of 2 cm (Figure 8a,8b) and 5 cm (Figure 8b,8d), respectively. From the figures, we can observe that the light can

be used to characterize individual fragment samples. Kruskal-Wallis test indicates no significant differences between all the plastic samples ( $\chi^2 = 10472.83$ ,  $\eta^2 = 0.99$ ,  $p < 0.05$ ). In addition, we can observe that the characterization of the samples changes slightly when it is performed from different distances. However, it is possible to see that the relative differences between different types of characterization are also preserved. Kolmogorov-Smirnov test to compare the relative differences in light reflectivity values from different distances verify that data is similar in both cases (KS=0.235,  $p > 0.05$ ). It is also possible to observe from the figure that the difference between samples is reduced as the distance increases, which implies that when the sensor is too far, detecting plastic fragments becomes infeasible. As a result, light sampling should be performed at least no further than 5 cm to guarantee good performance.

**Plastic fragment sample arrangement analysis:** We next quantify the amount of fragments that can be found in different contexts in the wild captured by TACO dataset. Figure 9a shows the results. From the figure, we can observe that most of the fragments are almost invisible for existing detection solutions. Indeed, around 90% of the cases in which micro or meso plastic is found include between 5 and 10 samples, which are also spread out across an area (dispersed case). Similarly, we can also observe a few cases (almost 10%) that has a significant amount of plastic fragments ( $> 15$  samples at once). Arrangements with lower amounts of plastic fragments are more challenging to analyze than higher ones as the presence of higher micro and meso plastic amounts can be already used as an indicator to mark an area for cleaning or removal procedures. Arrangements with lower amounts of plastic fragments can then be passed unnoticed for these procedures, polluting an ecosystem/space gradually until enough samples are accumulated over time to be detectable.

**Ratio analysis between plastic fragments and macro samples:** Plastic fragments are far from being isolated but rather, they are accompanied by macro size litter, which is likely to be its source as the macro litter degrades apart over time. Thus, next, we analyze the ratio relation between macro plastics and plastic fragments. Figure 12b shows the results. From the table, we can observe that in 25% images from the dataset, the ratio of plastic fragments to macro litter is 2 : 1. Similarly, for 50 percentile (median), the same ratio is 3 : 1 and for 75 percentile, the ratio is around 5 : 3 and the maximum number of fragments to macro is 82 : 13. Based on these analysis, we divided the image dataset into three categories. Category 1 includes images having litter distribution below 50 percentile, category 2 involves images lying between 50 percentile and 75 percentile and category 3 involves images above 75 percentile. Further analysis also reveals that 97% of the fragments are dispersed whereas only less than 3 percent can be categorized as agglomerated. This suggests that solutions like thermal imaging are totally ineffective to detect most of the fragments found in the wild.

**Individual modalities (baseline):** We next analyze the thermal dissipation times and light reflectivity values of the plastic

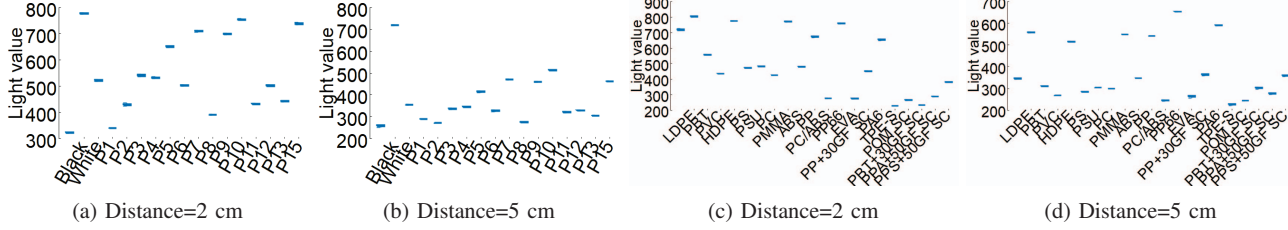


Fig. 8: Light reflectivity values: (a),(b) plastic fragments of different sizes; (c),(d) 20 different plastic fragment samples.

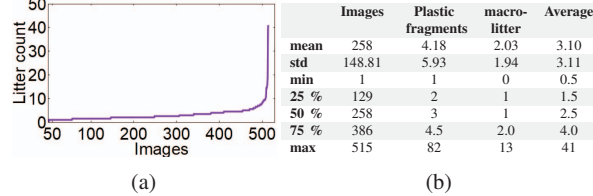


Fig. 9: Litter samples distribution. (a) Amount of plastic fragment samples identifiable in the wild (TACO dataset). (b) Litter distribution in extracted images

objects used in our experiments. Figure 10a shows the results of macro plastics detection using thermal imaging. From the results, we can observe that macro plastics provide relatively the same thermal dissipation time even when broken apart – even in different sizes. Kolmogorov-Smirnov test to compare the relative differences in thermal dissipation time between end plastic products and broken macro plastic parts (from the same products), verifies that both thermal dissipation characteristics are preserved ( $KS=0.141$ ,  $p > 0.05$ ). The main limitations of thermal imaging as a standalone solution, however, are limited resolution and the difficulty of inducing thermal radiation on small objects. As a result, LIZARD combines the two modalities to improve detection of smaller particles. In parallel, we derived light profiles from the end products by taking light measurements from different points along their surface. Figure 10b shows the results. The figure shows the light measurements for individual product to be contained within a small range and contain only little variation. This means that individual products can be characterized using light measurements only. The specific values are: Plastic bottle ( $1066.96 \pm 107.56$ ), Shampoo bottle ( $1734.06 \pm 202.97$ ) and Disposable plastic cup ( $2440.33 \pm 165.92$ ). However, light sensing requires sampling all locations and struggles in detecting which areas are contaminated by particles. These results suggest that, in general, both methods can serve as standalone solution but by combining them their effectiveness can be significantly improved by allowing them to focus only on specific parts of the detection.

**LIZARD performance:** We now analyze the performance of identifying macro plastics and plastic fragments using the arrangements extracted from real contexts. To do this, we located our samples in the locations extracted from the synthetic contexts, making it possible to apply our LIZARD sensing pipeline. Figure 11 shows the results of plastic fragment detection (as macro plastics are easily detectable). As the

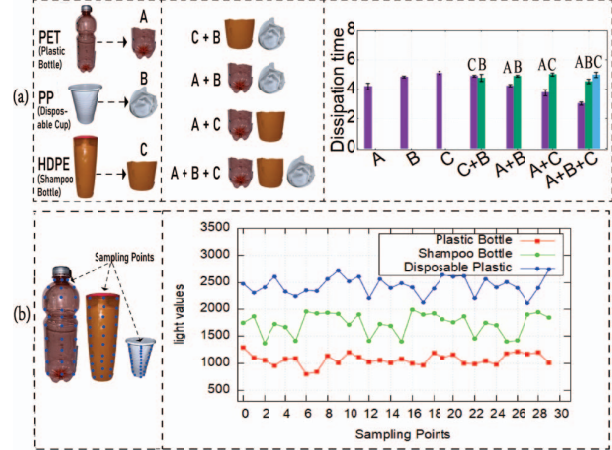


Fig. 10: Light reflectivity and thermal dissipation values of plastic samples, (a) thermal dissipation times for macro plastics, (b) Light reflectivity from different sampling points

background where the samples are located influences the overall result, we first analyze the effect of a fixed background for all the selected arrangements (Category-1, Category-2 and Category-3). A black background is used as a baseline. Kruskal-Wallis test between the light values of baseline background and different plastic fragment types and arrangements shows that plastic fragments can be differentiated from the background measurements ( $\chi^2 = 270.68$ , on average  $\eta^2 = 0.90$ ,  $p < 0.05$ ). For Category-1, we can observe from the results (Figures 11(a–c)) that 100% of plastic fragments are detected. Similarly, for Category-2 (Figures 11: d–f), plastic fragment detection also reached about 100%. Category-1 and Category-2 have low distribution of plastic fragments (below 75 percentile), and we rely on Type-2 and Type-3 fragments mostly. As a result, all of the fragments were detected. After that, we analyze the Category-3 arrangement (Figures 11(g–i)), which has a litter distribution above 75 percentile. For this category, the overall accuracy is up to 89%. The decline in accuracy for plastic fragment detection is that we increase the amount of Type-1 plastics (less than 5 mm) in the arrangement. This suggests that the plastic samples (Type-1) are difficult to detect in some cases. Figure 12a summarizes the number of plastic samples detected by LIZARD versus the number of plastic samples that are actually present in the selected arrangements. Our results indicate that a single area mapping is insufficient to detect all different types of plastic fragments as it retrieves only accurate results for the bigger plastic fragments. Thus, the area should be mapped multiple times to identify micro and

meso plastics robustly. Since our LIZARD methods already reduce the mapping area to find micro and meso plastics, it makes it suitable for exploring an area multiple times without introducing much overhead in the sampling.

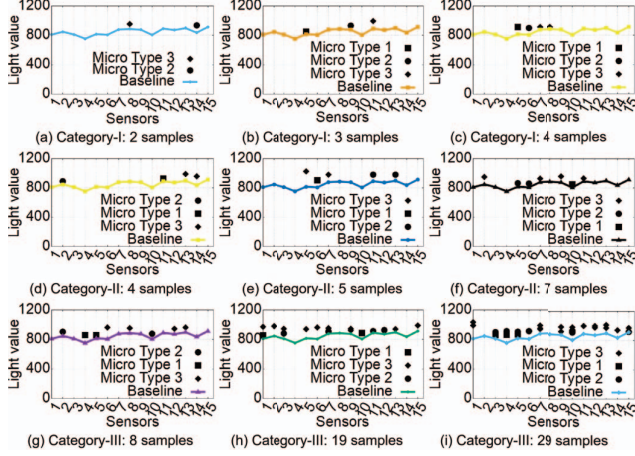


Fig. 11: Light reflectivity for different categories.

**LIZARD performance on more realistic background:** Besides using the black generic background as a baseline for plastic fragment detection, we also analyze the performance of our method when using more realistic backgrounds found in public areas. From the TACO dataset analysis, we found that the most common (contextual) backgrounds where litter is present are concrete, sand, soil, wood and grass. Bumpy background was also used for evaluation. We first present baseline light values of backgrounds without plastic samples in Figure 12(c-d). As expected, some light backgrounds show more variation in light values than others. Thus, we consider these additional backgrounds in our experiments. Figure 13 shows the results of light reflectivity values when considering the different backgrounds. Kruskal-Wallis test between the light values of backgrounds and different plastic fragment types indicates that the values are statistically significant ( $\chi^2 = 89.5$  to  $120.0$ ,  $\eta^2 = 0.85$ ,  $p < 0.05$ ). This suggests that there are differences between light measurements of the plastic fragment samples and the background location. Thus, it is possible to separate the micro samples from the background where the samples are located. This can be seen further in Figure 12b, where we demonstrate the light value of specific plastic fragments in different contexts. From the figure, we can observe that the light value of plastic samples have small variations. The mean and standard deviation of light reflectivity values for Type 1 fragments in all backgrounds is  $869 \pm 31.54$ , that of Type 2 is  $924.28 \pm 9.81$  and for Type 3 is  $992.28 \pm 29.24$  respectively. Figure 13f shows how background deformations (bumpy ground) influence the performance. We can observe that the detection is preserved even though there are a lot of fluctuations in light values due to the background bumpiness (deformations). Kruskal-Wallis test using light values in bumpy background and different fragments indicates that the values are statistically significant ( $\chi^2 = 118.5$ ,  $\eta^2 = 0.883$ ,  $p < 0.05$ ).

**Classification performance:** We first perform k-means clustering algorithm on the light values of different plastic samples with number of clusters equal to 3 to demonstrate the light values of the three different types of plastic samples fall into individual groups. Figure 14a shows the results. As we can see from the results, the plastic fragment types are more easier to detect when using a black background. The three black circles show the centroids of the three clusters which are quite differentiated from each other. The centroid of cluster 1 (Type 1) lies at 870; for cluster 2 at 914 and for cluster 3 at 970. When analyzing the influence of more realistic background, the values are spread. This happens in cases where the background color is lighter, e.g., polished wood, sand, as more light from the diode is reflected back to the photoresistor. In other words, the light values can vary depending on their background location. Thus, background is a important factor to consider when classifying plastic samples. We then construct a classical machine learning model using this information. We used One Hot Encoding to preprocess the categorical background. The 10 fold cross validation score was around 77% to 80% when we used RF classifier. The same score was found to be around 70 to 75 percent with SVM classifier.

**Comparison to baseline:** LIZARD performance is compared against visual inspection, which is the most common method for identification and removal of plastic fragments [8]. Other methods require bulky, expensive, and complex deployment of instruments to detect them, making them unsuitable for large-scale usage. Visual inspection can at least be applied in a variety of different contexts when compared to advanced methods. Unlike others, LIZARD requires partial (or none) human-support and can be also envisioned to improve the accuracy of the inspection performed by naked eye. We established the comparison baseline by designing a user study that quantifies human performance to identify plastic fragments. Thus, we designed a testbed where different locations (backgrounds) are evaluated. We selected Sand, Grass and Rocky backgrounds, which match our main evaluation of our proposed method. We rely on Category-3 arrangement as it contains the larger amount (29 plastic fragments) of plastic fragments that are realistically found in the wild. The arrangement was mapped to a  $20 \times 14$  cm area and contains micro (9), meso (13) and macro (7) plastics (See Figure 14b). 45 (15 per location) participants from University campus are surveyed. Participants were randomly asked to perform the task while walking through the campus and no personal data is collected. The task was to remove all plastic fragments from the testbed location that could be identified and stopped once they thought the location was clean of fragments. A stopwatch and an android application are used to record timestamps between removed plastic fragments.

**Comparison results:** Figure 14c shows the results. From the figure, we can observe that at the start of the experiment, plastic fragments are removed quickly. On average for all the locations, 18 fragments of plastic are removed at a rate of 20s before the time increases exponentially. The average time of each location

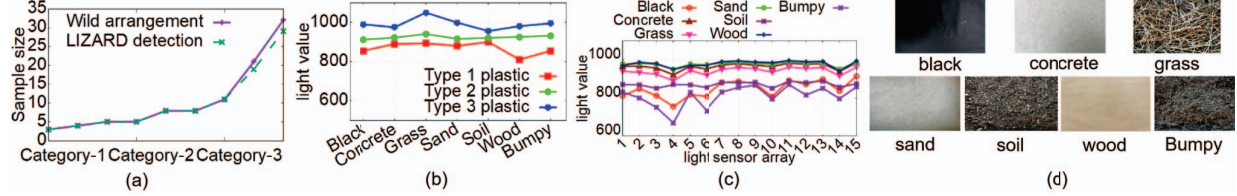


Fig. 12: a) Comparison with ground truth b) Light values of same plastic fragments in different contexts, c)-d): Baseline light reflectivity of different backgrounds.

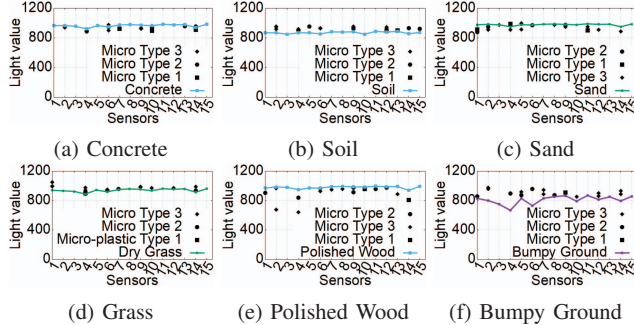


Fig. 13: Light reflectivity values of plastic samples.

is, Sand=70.4 s, Rock=81.04 s and Grass=113 s, demonstrating that location is a factor that influences visual performance. In terms of removal performance, 92% of samples were removed from sand, 86% from Rock, and 76% from Grass, re-enforcing that plastic fragments are difficult to remove entirely from the environment. When compared to the baseline, we can observe that LIZARD provides better removal performance (up to 98%) and the time of identification overperforms human visual inspection.

## VI. REAL-WORLD PRACTICABILITY

Our experiments showed promising results with real-world litter footage but didn't demonstrate its performance in the actual environment. In this section, we demonstrate LIZARD robustness in real-world environments.

**Experimental setup:** LIZARD was evaluated in three different locations with different backgrounds: soil (park), gravel, and cast iron (manhole cover). Figures 15 show the LIZARD deployment in detail. The experiment was conducted for 5 days at different times (morning, afternoon, and night), so it was possible to analyze different luminosity conditions.

**Procedure:** We selected an arrangement of 15 plastics samples that contain the three types of plastics evaluated previously: 4 type 1 (i.e., micro plastics <5mm), 6 type-2 (i.e., meso plastics 5mm - 1.5cm) and 5 type-3 (i.e., macro plastic fragments >1.5cm) samples. We use light reflectivity in LIZARD to detect the different fragment types. We also collect ambient luminosity using the LUX Meter Application.

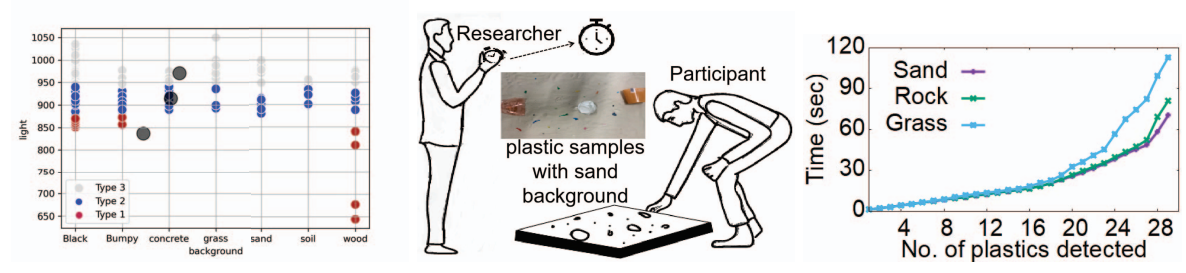
**LIZARD performance:** Figure 16(a-c) shows the luminosity values for the different backgrounds as measured by the LUX Meter Application and Figure 16(d-f) characterizes the backgrounds where the plastic fragments were located. The background locations have distinctive profiles with the gravel resulting in highest variations due to the uneven nature

of the surface. The background characteristics also change significantly based on luminosity with morning and afternoon differing from the night measurements. Figure 17 shows the light intensity values for different plastics at different times of day. The results mirror our controlled evaluation, demonstrating that all plastic fragments can be recognized, even if there is slight drop in performance as the surfaces are uneven and as the luminosity changes over time. The best results are obtained during morning and afternoon where ambient sunlight affects the sensors, and the worst during night. Note that this could be compensated by integrating the AGV with a separate light source. The main errors occur between types-2 and 3, i.e., the micro plastics can be easily distinguished and most errors occur between meso and macro plastic fragments. We also performed statistical testing to verify that the data captured from the real-world environments matches those obtained in the controlled tests. The closest match in backgrounds is between the soil category, and we thus focus on comparing the measurements in the soil condition between the two experiments. We perform a Kolmogorov-Smirnov test between these two, verifying that the data is similar in both cases ( $KS=0.428$ ,  $p > 0.05$ ). Finally, we evaluate the classification performance of LIZARD considering the data collected from the light. Note that unlike controlled experiments, which were conducted under constant luminosity conditions, the data obtained from real-world deployments encompasses various luminosity values. Upon incorporating luminosity as an input feature, the overall accuracy of the model improved to around 85% (Figure 18).

## VII. RELATED WORK

Table I shows a summary of relevant work that investigates the identification of litter, and the use of personal and autonomous devices to achieve it.

**Pervasive sensing:** Different smartphone sensors have been re-purposed to identify materials and evaluate their inherent properties on the spot [22], [13]. Determining sugar content in liquids has been explored using near-infrared sensors [23]. Soil and moisture salinity has been explored through wireless signals [24]. Characterization of liquids using wireless also has been explored [25]. Several other sensors have been used for liquid characterization, e.g., acoustic [26], vibration [27], and light sensors [28]. Optical sensing has also been adopted, e.g., to measure water quality [29], to characterize underwater waste [30], and to detect ripeness of organic produce [31]. Cameras have been used extensively to analyze liquid's tensions [32] and identify materials via material reflection [33]. RFID stickers have been used to learn the quality of food [34].



(a) Clustering of types

Fig. 14: (a) k-means clustering, b)-c) Removal of plastic fragments via visual inspection.

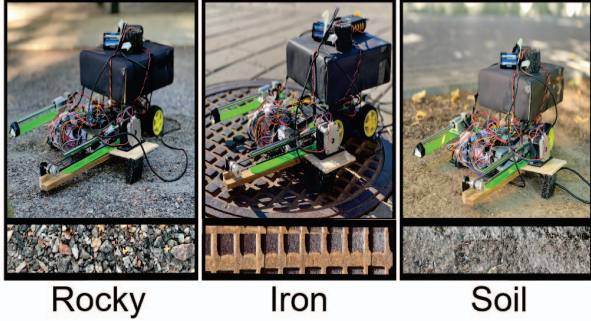


Fig. 15: LIZARD deployment in different locations

Near-infrared spectroscopy devices have been developed to identify medical pills [35], non-invasive blood glucose level monitoring [36], and brain activity monitoring [37]. Near-infrared spectroscopy is also used to estimate the quality of fruits [38]. Thermal imaging also has been proposed to detect different material types [39]. Unlike others, our work combines different sensing modalities to identify plastics at different size scales, including, meso, micro and nano.

**Plastic identification:** Manual cleaning campaigns have been adopted as a solution to overcome the litter removal problem. Automated solutions also have been developed to tackle the problem. Computer vision methods (object recognition) are the most common autonomous approaches to identify plastics [1]. Methods for identifying plastics in oceans [40] and removing plastic litter from public spaces [41] at macro level have been investigated. Optical solutions have been studied to identify different types of plastics underwater [14], [42]. Macro-plastics (more than 200 mm in size) are easy to detect by the human eye [43]. Despite several approaches available to detect plastics, a key problem that has been partially overcome is the detection of micro-plastics. Indeed, unlike macro plastics, the micro plastics (< 5mm in size) are difficult to detect due to their size. Microplastics are generated through the degradation of macro and meso plastics, as they break down in response to environmental conditions. [11]. The most common method to detect micro plastics are based on spectroscopy techniques, like fourier transformation infrared spectroscopy (FTIR) and Raman spectroscopy [7]. While these methods are highly accurate, they can only be utilized in controlled environments. Moreover, these methods are expensive and require bulky instruments. Thus, they cannot be applied in the wild contexts or integrated

Ref	Plastic size	Integration with AV	Techniques	Area Mapping	Off-the-shelf components
[39]	Macro	No	Ambient Light	Full	Yes
[13]	Macro	Yes	Human touch	Partial	Yes
[14]	Macro	Yes	Sunlight	Full	Yes
[44]	Macro	No	Object recognition	Full	No
[45]	Macro	No	Sunlight	Full	No
[41]	Macro	Yes	Object recognition	Full	No
[1]	Macro	No	Object recognition	Full	No
[46]	Macro	No	Object recognition	Full	No
[2]	Macro	No	Object recognition	Full	No
[47]	Macro	No	Object recognition	Full	No
[48]	Macro	No	Object recognition	Full	No
[49]	Macro	Yes	Object recognition	Full	No
[42]	Macro	Yes	Light	Full	Yes
[30]	Macro	Yes	Light	Full	Yes
[33]	Macro	No	Light	Full	Yes
[50]	Micro	No	Light	Full	No
Our work	Macro & Micro	Yes	Light	Partial	Yes

TABLE I: State-of-the-art for identification of plastics and potential integration with autonomous vehicles (AV).

into autonomous vehicles with ease. Our work explores the identification of different plastic particles in the wild, affected by different environmental factors, e.g., sunlight, and different surfaces. Moreover, we also demonstrate how our solutions can be integrated into autonomous ground vehicles.

## VIII. DISCUSSION

**Stakeholders and Adoption:** The experiments demonstrated that LIZARD is a promising solution for identifying macro, meso, and micro litter in the environment. This capability to obtain information about different litter particle sizes is the key feature setting LIZARD apart from existing solutions. Naturally, the accuracy of LIZARD is lower than with dedicated scientific instruments, such as FTIR or Infared microscopy, and thus the main use for LIZARD is to use it to autonomously identify areas that are badly affected and to help coordinate cleaning efforts. Another possible use would be to integrate it as part of drones that are operating within a city (e.g., delivery drones).

**Context and sensor calibration:** A limitation of our technique is background influence on micro-particle detection. Darker backgrounds (e.g., soil) ease detection as they reflect less light than lighter backgrounds (e.g., sand). Overall, our results were promising even with varying backgrounds. Highly reflective ground might benefit from more advanced sensor designs, such as using a small array of light sources to project a pattern for material estimation. Other options involve closer sensor placement or models considering background material. We are

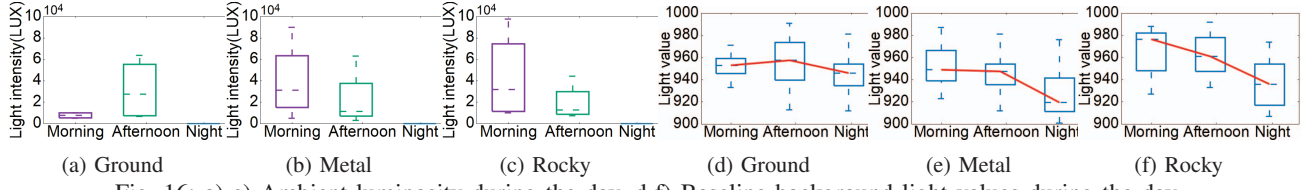


Fig. 16: a-c) Ambient luminosity during the day, d-f) Baseline background light values during the day.

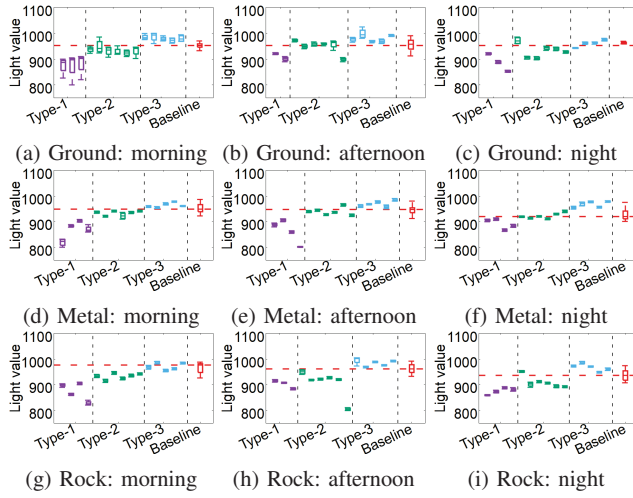


Fig. 17: Plastic fragment detection in the Wild

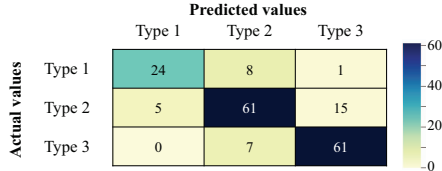


Fig. 18: Improvement on classification accuracy.

also interested in nighttime applications, leveraging consistent lighting, often from onboard AGVs, in low-light conditions.

**Environmental Adaptability:** Rain and snow can challenge micro-particle detection, but our solution remains reliable for macro particles, leveraging thermal imaging's environmental insensitivity. While it offers insights into potential micro-particle locations, accuracy may be reduced. To address these, we can explore extendable covers to counteract weather effects and reflections. LIZARD uses thermal imaging for macro-plastic detection, acknowledging the impact of weather conditions. Shielding the thermal camera is a potential remedy. In aquatic or aerial settings, computer vision provides an alternative. For instance, LIZARD can identify plastic fragments in water, complementing established methods. While integration with underwater drones is feasible, it requires thoughtful design. However, implementing computer vision on resource-constrained devices demands extra resources.

**On energy consumption:** LIZARD adds sensors to AGVs with minimal operational impact. Unlike underwater and aerial vehicles, AGVs handle extra weight better, without navigation instability or increased energy use. In our experiments,

LIZARD's added weight doesn't burden AGVs, avoiding extra energy consumption. AGV sensors include their own batteries, adding to the total weight. We opt for classical machine learning for classification, as deep learning, requiring ample data, proves resource-intensive for constrained devices [51].

**AGV Integration:** The experimental prototype combined off-the-shelf components and an affordable AGV. Integration challenges need to be addressed for larger-scale operations. The sensing units have their own power sources and don't affect the AGV's resource consumption. Plastic recognition uses a smartphone with a thermal camera and a sunshield, adding 350 grams. Additional light sensors and batteries add 50 grams. The total payload is 400 grams. This has indirect effects on energy [52] and may require re-calibration for navigation [53]. Future drones are expected to be modular. Currently, integration is difficult. Light sensors and a stepper motor are placed on the front of the AGV, requiring weight compensation at the back. Re-configurable components can overcome this issue.

## IX. SUMMARY AND CONCLUSIONS

In this paper, we presented LIZARD, an innovative pervasive sensing method that detects plastic fragments located in the environment. Plastic fragments are difficult to detect due to their small size and effort required to sample an area. LIZARD relies on two sensing modalities to detect such fragments, thermal imaging and light reflectivity. LIZARD has been designed to be integrated into AGVs, such that it is possible to monitor continuously public spaces and natural ecosystems. We designed a proof-of-concept AGV that is equipped with LIZARD to evaluate the feasibility of our solution. Through rigorous experiments that consider different realistic situations and environments, we found that our method is capable to detect plastic fragments with an accuracy up to 80%. When compared with existing solution, our method is the first of its kind that enables the detection of plastic fragments using autonomous technologies. Our work paves the way towards new pervasive solutions to foster environmental sustainability.

## ACKNOWLEDGMENT

This research has been financed by European Social Fund via "ICT programme" measure, the Academy of Finland project 339614 and the Nokia Foundation (grant number: 20220138), the European Research Council (ERC) under the European Union's Horizon 2020 research and innovation program, grant agreement No 948666 – ERC-2020-StG NaPuE, the University of Helsinki (Three-Year Research Grant), MUR Bando FARE Ricerca in Italia project NATtA (R20T85832Z).

## REFERENCES

- [1] J. Bobulski and M. Kubanek, "Waste classification system using image processing and convolutional neural networks," in *International workshop conference on artificial neural networks*. Springer, 2019, pp. 350–361.
- [2] J. Lorenzo-Navarro *et al.*, "Smacc: a system for microplastics automatic counting and classification," *IEEE Access*, vol. 8, pp. 25 249–25 261, 2020.
- [3] de Souza Machado *et al.*, "Microplastics as an emerging threat to terrestrial ecosystems," *Global change biology*, vol. 24, no. 4, pp. 1405–1416, 2018.
- [4] J.-Q. Jiang, "Occurrence of microplastics and its pollution in the environment: A review," *Sustainable production and consumption*, vol. 13, pp. 16–23, 2018.
- [5] L. Wang *et al.*, "Birds and plastic pollution: recent advances," *Avian Research*, vol. 12, no. 1, pp. 1–9, 2021.
- [6] F. Ribeiro *et al.*, "Accumulation and fate of nano-and micro-plastics and associated contaminants in organisms," *TrAC*, vol. 111, pp. 139–147, 2019.
- [7] I. N. P *et al.*, "Microplastic in aquatic ecosystems," *Angewandte Chemie International Edition*, vol. 56, no. 7, pp. 1720–1739, 2017.
- [8] P. G. Ryan *et al.*, "Monitoring the abundance of plastic debris in the marine environment," *Philosophical Transactions B*, vol. 364, no. 1526, pp. 1999–2012, 2009.
- [9] G. A. Tobin *et al.*, "The effectiveness of street sweepers in removing pollutants from road surfaces in florida," *J Environ Sci Health*, vol. 37, no. 9, pp. 1687–1700, 2002.
- [10] H.-S. Lo *et al.*, "Field test of beach litter assessment by commercial aerial drone," *Marine Pollution Bulletin*, vol. 151, p. 110823, 2020.
- [11] M. Padervand *et al.*, "Removal of microplastics from the environment. a review," *Environmental Chemistry Letters*, vol. 18, no. 3, pp. 807–828, 2020.
- [12] Aral *et al.*, "Classification of trashnet dataset based on deep learning models," in *2018 IEEE (Big Data)*. IEEE, 2018, pp. 2058–2062.
- [13] Emenike *et al.*, "Characterizing everyday objects using human touch: Thermal dissipation as a sensing modality," in *2021 IEEE PerCom*. IEEE, 2021, pp. 1–8.
- [14] Z. Yin *et al.*, "Toward city-scale litter monitoring using autonomous ground vehicles," *IEEE Pervasive Computing*, 2022.
- [15] M. Rinta-Homi *et al.*, "How low can you go? performance trade-offs in low-resolution thermal sensors for occupancy detection: A systematic evaluation," *IMWUT*, vol. 5, no. 3, pp. 1–22, 2021.
- [16] J.-Y. Wu *et al.*, "Mrim: Enabling mixed-resolution imaging for low-power pervasive vision tasks," in *2022 Percom*. IEEE, 2022, pp. 44–53.
- [17] G. Lee, R. Gommers, F. Waselewski, K. Wohlfahrt, and A. O'Leary, "Pywavelets: A python package for wavelet analysis," *Journal of Open Source Software*, vol. 4, no. 36, p. 1237, 2019.
- [18] M. Hushchyn and A. Ustyuzhanin, "Generalization of change-point detection in time series data based on direct density ratio estimation," *Journal of Computational Science*, vol. 53, p. 101385, 2021.
- [19] Bianco *et al.*, "Atmospheric transport of micro and nanoplastics and fluorescence detection of particles; 20  $\mu\text{m}$ ," in *EGU*, 2021, pp. EGU21-3914.
- [20] A. L. Andrade, "The plastic in microplastics: A review," *Marine pollution bulletin*, vol. 119, no. 1, pp. 12–22, 2017.
- [21] "Taco - open image dataset of waste in the wild." <http://tacodataset.org/>, 2022.
- [22] C. Wu *et al.*, "msense: Towards mobile material sensing with a single millimeter-wave radio," *IMWUT*, vol. 4, no. 3, pp. 1–20, 2020.
- [23] J. Weiwei *et al.*, "Probing sucrose contents in everyday drinks using miniaturized near-infrared spectroscopy scanners," *IMWUT*, vol. 3, no. 4, pp. 1–25, 2019.
- [24] W. Yang *et al.*, "Wi-wheat: Contact-free wheat moisture detection with commodity wifi," in *2018 IEEE ICC*. IEEE, 2018, pp. 1–6.
- [25] Dhekne *et al.*, "Liquid: A wireless liquid identifier," in *Proceedings of the 16th AIC on Mobile Systems, Applications, and Services*. ACM, 2018, pp. 442–454.
- [26] Y. Yang *et al.*, "Hearliquid: Non-intrusive liquid fraud detection using commodity acoustic devices," *IEEE Internet of Things Journal*, 2022.
- [27] H. Yongzhi *et al.*, "A portable and convenient system for unknown liquid identification with smartphone vibration," *IEEE TMC*, 2021.
- [28] Huang *et al.*, "Lili: liquor quality monitoring based on light signals," in *Proceedings of the 27th Annual Mobicom*, 2021, pp. 256–268.
- [29] P. N. J. Fernandez, "Using a low-cost green light emitting diode to measure total suspended solids in a marine protected area of the philippines," *Journal of Coastal Research*, vol. 38, no. 1, pp. 99–113, 2022.
- [30] F. Huber *et al.*, "Penguin: aquatic plastic pollution sensing using auvs," in *DroNet@ MobiSys*, 2020, pp. 5–1.
- [31] A. Zuniga *et al.*, "Ripe or rotten? low-cost produce quality estimation using reflective green light sensing," *IEEE PerCom*, vol. 20, no. 3, pp. 60–67, 2021.
- [32] S. Yue *et al.*, "Liquid testing with your smartphone," in *IMWUT*. ACM, 2019, pp. 275–286.
- [33] H.-S. Yeo *et al.*, "Specam: sensing surface color and material with the front-facing camera of a mobile device," in *MOBILEHCI*. ACM, 2017, p. 25.
- [34] U. Ha, Y. Ma *et al.*, "Learning food quality and safety from wireless stickers," in *HotNets*, 2018, pp. 106–112.
- [35] K. Simon *et al.*, "Assisted medication management in elderly care using miniaturised near-infrared spectroscopy," *IMWUT*, vol. 2, no. 2, p. 69, 2018.
- [36] L. Tang *et al.*, "Non-invasive blood glucose monitoring technology: a review," *Sensors*, vol. 20, no. 23, p. 6925, 2020.
- [37] K. H. Yeong *et al.*, "Application of functional near-infrared spectroscopy to the study of brain function in humans and animal models," *Molecules and cells*, vol. 40, no. 8, p. 523, 2017.
- [38] Y. Shao *et al.*, "Near-infrared spectroscopy for classification of oranges and prediction of the sugar content," *IJFP*, vol. 12, no. 3, pp. 644–658, 2009.
- [39] Cho *et al.*, "Proximate material type recognition in the wild through deep learning of spatial surface temperature patterns," in *ACM CHI*. ACM, 2018, p. 2.
- [40] Araujo *et al.*, "Identification of microplastics using raman spectroscopy: Latest developments and future prospects," *Water research*, vol. 142, pp. 426–440, 2018.
- [41] J. Su *et al.*, "Design of litter collection robot for urban environment," in *Intl. Mechanical Engineering Congress and Exposition*, vol. 85611. ASME, 2021, p. V07AT07A018.
- [42] F. Huber *et al.*, "Toward large-scale autonomous marine pollution monitoring," *IEEE Internet of Things Magazine*, vol. 4, no. 1, pp. 40–45, 2021.
- [43] Eriksen *et al.*, "Microplastic pollution in the surface waters of the Laurentian great lakes," *Marine pollution bulletin*, vol. 77, no. 1-2, pp. 177–182, 2013.
- [44] M. Radeta *et al.*, "Deep learning and the oceans," *Computer: a publication of the IEEE Computer Society*, 2022.
- [45] L. Goddijn-Murphy *et al.*, "On thermal infrared remote sensing of plastic pollution in natural waters," *Remote Sensing*, vol. 11, no. 18, p. 2159, 2019.
- [46] A. N. Kokoulin *et al.*, "Convolutional neural networks application in plastic waste recognition and sorting," in *IEEE EICONRUS*. IEEE, 2018, pp. 1094–1098.
- [47] M. W. Rahman *et al.*, "Intelligent waste management system using deep learning with iot," *JKSUCI*, 2020.
- [48] G. White, C. Cabrera, A. Palade, F. Li, and S. Clarke, "Wastenet: Waste classification at the edge for smart bins," *arXiv preprint arXiv:2006.05873*, 2020.
- [49] M. Wolf *et al.*, "Machine learning for aquatic plastic litter detection, classification and quantification (aplastic-q)," *Environmental Research Letters*, vol. 15, no. 11, p. 114042, 2020.
- [50] Z. Zhu *et al.*, "Plasticnet: Deep learning for automatic microplastic recognition via ft-ir spectroscopy," *JCVIS*, vol. 6, no. 1, pp. 1–3, 2020.
- [51] T. Pulkkinen *et al.*, "Understanding wifi cross-technology interference detection in the real world," in *2020 IEEE 40th ICDCS*. IEEE, 2020, pp. 954–964.
- [52] M. Liyanage *et al.*, "Geese: Edge computing enabled by uavs," *Pervasive and Mobile Computing*, vol. 72, p. 101340, 2021.
- [53] M. Triananda *et al.*, "Analysis of effect of center of gravity change towards type m1 vehicle stability," in *AIP Conference Proceedings*, vol. 2376, no. 1. AIP Publishing LLC, 2021, p. 070013.